

# DESIGN OF POWER TRACKING MODEL FOR PHOTOVOLTAIC POWER GENERATION BASED ON IMPROVED QUANTUM SWARM ALGORITHM AND CONDUCTANCE INCREMENTAL APPROACH

Xuemei Yang,\* Wenqing Zhang,\* and Wenwen Zou\*

## Abstract

This paper suggests a novel photovoltaic (PV) power tracking model to address the limitations of maximum power point tracking (MPPT) to fully utilise renewable resources like solar energy. The model is based on the quantum swarm algorithm (QSA), which is enhanced by the fuzzy logic (FL) algorithm to speed up optimisation and ensure optimisation accuracy, along with the conductivity incremental method, which is enhanced by the variable step-size algorithm to guarantee convergence of the algorithm. The purpose of simulation experiments is to validate the model's viability. According to the experimental findings, the upgraded genetic gene algorithm discovered the maximum electric power point at 2,034 W, while the improved quantum swarm method found the greatest electric power point at 2,920 W. The tracking speed was increased by 21.95% compared to the simulation results (SR) of the original conductivity incremental technique, which were 0.41 s and 0.32 s, respectively. The light intensity was increased from 200 W/m<sup>2</sup> to 400 W/m<sup>2</sup>. The SR are 0.46 s and 0.38 s, respectively, and the tracking speed is enhanced by 17.39%. The average output power of the PV arrays is 41.52 W and 39.86 W, respectively. The tracking rate can be increased by 15% to 25% using the enhanced conductivity increment approach. It is clear that this study method has enhanced and ensured the tracking speed and accuracy of the maximum power of PV power generation, which has the practical value of energy conservation and maximising the use of solar energy resources.

## Key Words

Photovoltaic power system, maximum power tracking, fuzzy logic, quantum swarm algorithm, conductance increment method

\* Wuwei Power Supply Company, State Grid Gansu Electric Power Company, Wuwei 733000, China; e-mail: zww18419519093@163.com  
Corresponding author: Wenwen Zou

*Recommended by Shuhui Li*  
(DOI: 10.2316/J.2024.203-0532)

## 1. Introduction

Maximum power point tracking (MPPT) technology for PV power generation is significantly enhanced using quantum swarm algorithm (QSA), which is superior to particle swarm algorithm. The particle swarm optimisation technique QSA, which is based on quantum computation, has the drawbacks of being simple to fall into local optimisation and having a sluggish process for searching for optimisations. Since then, the fuzzy logic (FL) algorithm has been introduced. The FL algorithm will transform the input fuzzy data into fuzzified and defuzzified data, and then produce fuzzy data. The algorithm can address the issues of local optimisation and slow QSA algorithm rate since it is quick and compatible. The variable step algorithm works in conjunction with the conductance increment method (CIM) to directly and continuously regulate the duty cycle. The variable step algorithm is a widely used algorithm for photovoltaic (PV) power tracking technology. It finds the maximum power point (MPP) by varying the solar cell's output voltage, but it also has a slow convergence rate. Based on the foregoing, an improved PV power tracking model with QSA and CIM is proposed to increase tracking rate, guarantee algorithmic optimisation accuracy, and enable simple adjustment of converter duty cycle to achieve high efficiency and accuracy of the MPPT to achieve full utilisation of solar resources. The basic structure of the study paper is as follows: The history and relevance of the study on PV power tracking are presented in the first section; the second section discusses the innovation and challenge of this research and describes how to improve and optimise QSA and CIM as well as the optimisation process of the associated algorithm model; the third section designs a simulation experiment and evaluates and verifies the model's viability and applicability based on the experiment.

## 2. Related Works

Solar energy, a novel form of energy, is the finest option for energy conservation in the modern world to rationalise and utilise energy to the fullest extent possible. To employ PV cells as efficiently as possible, or to acquire the greatest power for use in current technology, experts have presented solutions. PV cells are frequently used devices to convert solar energy into electrical energy. Dagal *et al.* researched a particle swarm optimisation-based enhanced Salp swarm method for optimising a PV system's MPPT. The PV Solarex-MSX-60 PV solar panel is used with the Salp swarm method for particle swarm optimisation and is chosen based on the parameters of the suggested algorithm taking voltage [1]. Partial shading was cited by Mao L as a serious flaw in the design of the current MPPT controllers. He suggested using the new slime mould optimise (SMO) and improved Salp swarm algorithm (ISSA) MPPT controllers to track GMPP for various PV array layouts. Dyad-based learning and local search algorithms (LSA) are used by ISSA to maximise the search space's exploration [2]. To eliminate the computational overhead and drift impact, the Manoharan team suggested a straightforward and improved P&O MPPT technique. The effectiveness of the suggested method is evaluated using a typical boost converter, and the direct duty cycle technique is used to confirm its efficacy [3]. Muhammad Ali in light of the dramatic improvement in PV efficiency, a robust improved perturb and observe MPPT method is developed. The small-step search zone is reduced to 15% of the whole PV operating region by the proposed tracking method, which reduces the need for lengthy small-step iterations [4].

A new MPPT technique is proposed by Xu *et al.* to address the issue that the conventional incremental conductance (INC) algorithm has a low response speed under fast changes in solar radiation level or load resistance because of its fixed step size [5]. A quick, effective, linear incremental conductance (IC) approach was put out by Siddique *et al.* to track the MPP of a grid-connected PV array. Switches are fewer in number for the best power generation. A thorough design of the PV converter system is integrated with the analysis of several MPPT approaches [6]. For PV systems, Mishra *et al.* suggested an auto-tuned IC MPPT algorithm. In terms of MPPT perturbation frequency and step size in response to changes in PV voltage, the proposed MPPT algorithm is intrinsically adaptive [7]. A new automated design of PV MPPT based on robust sliding mode control using an automated programmable logic controller was proposed by Ouberri (PLC) software. By continuously monitoring the MPP and greatly reducing oscillations, the goal is to maintain maximum PV system performance while overcoming the limitations typically associated with conventional MPPT algorithms when employing automated PLCs [8].

In summary, for the MPPT problem, it is divided into two improvement directions, particle swarm algorithm to find the optimal as well as CIM. Scholars mostly improve the step size and optimise the correlation coefficient of CIM, and a few of them adopt particle swarm optimisation

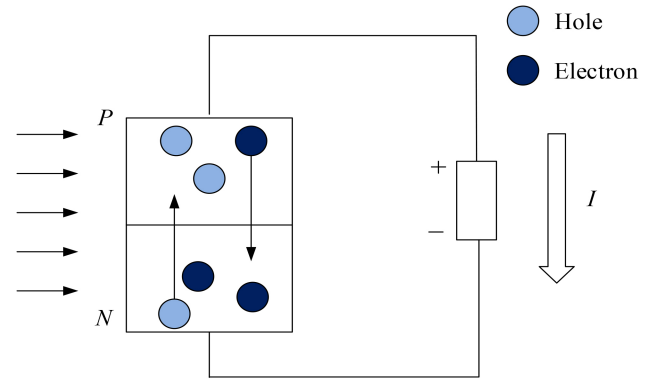


Figure 1. Schematic diagram of the utility of the photovoltaic principle.

algorithm for algorithmic optimisation. However, the algorithm improvement in two aspects is not deep enough, and there are few researches on improving the accuracy of MPPT technology by combining the two algorithms. The QSA, which outperforms the particle swarm algorithm, and the CIM, which has a better step size, are combined to create a new type of PV power tracking model in this study.

## 3. Tracking Model for Photovoltaic Power Generation Based on Improved QSA and CIM

A novel PV power tracking model is proposed by fusing the enhanced QSA with CIM to guarantee the tracking rate and accuracy of the MPPT points of PV power generation and to facilitate easy modification of the duty cycle when the light changes.

### 3.1 Characteristics of the PV Cells and Point Tracking Technology for Power Generation

The conversion of light energy into electricity is a major characteristic of PV cells, the sunlight will be irradiated to the PV panel, the PV panel will be collected a small amount of photons, in the semiconductor surface of the panel to produce the electronic empty pair of holes, for the PV principle [9]. The separation of electron-hole pairs occurs through the action of an electric field, causing the holes to move towards the *P*-terminal and the electrons to move towards the *N*-terminal. This creates a potential difference, which in turn creates an electric current. The utility of the PV principle is illustrated in Fig. 1.

The principle of PV cells can be shown mathematically, and the equivalent circuits of PV cells are most typically single diode and double diode circuits [10]. Which carries out the most stable and accurate results of the PV effect. Figure 2 depicts the equivalent circuit of the double diode used in this investigation.

According to Kirchhoff's current effect, the output side of the circuit voltage is obtained as in (1).

$$I = I_{pv} - I_{d1} - I_{d2} - \left( \frac{V + IR_s}{R_p} \right) \quad (1)$$

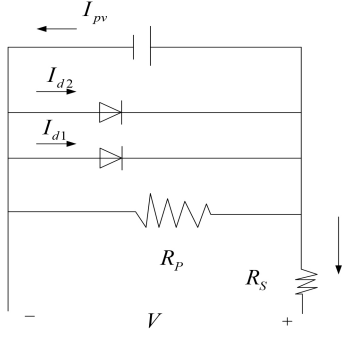


Figure 2. Dual diode equivalent model for photovoltaic cells.

Where  $I_{d1}$  is calculated as in (2).

$$\begin{cases} I = -(I_{d1} + I_{d2} - I_{pv}) - \left(\frac{V+IR_s}{R_p}\right) \\ I_{d1} = I_{O2} \left[ \exp\left(\frac{V+IR_s}{a_2 V_{T2}}\right) - 1 \right] \end{cases} \quad (2)$$

To maintain a certain level of accuracy, but to reduce the amount of computation involved, the model is simplified somewhat as in (3).

$$I = I_{PV} - I_O \left[ \exp\left(\frac{U + (N_S/N_P) IR_S}{a N_S V_T}\right) - 1 \right] - \frac{U + \left(\frac{N_S}{N_P}\right) IR_S}{\left(\frac{N_S}{N_P}\right) R_P} \quad (3)$$

In (3)  $I_{PV}$  represents the output voltage value,  $I$  represents the output current value,  $R_P$  represents the parallel resistor resistance of the equivalent parallel circuit,  $R_S$  represents the series resistor resistance,  $N_S$  represents the number of parallel modules,  $I_{PV}$  represents the current generated by the photogenerated circuit,  $N_P$  represents the number of series modules,  $a$  represents the ideal factor, and  $a$  represents the saturation current in the reverse direction. The relevant calculations for  $I_{PV}$  and  $a$  are shown in (4).

$$\begin{cases} I_{PV} = N_P (K_i \Delta T + I_{sc\_STC}) \frac{S}{S_{STC}} \\ I_O = N_P (K_i \Delta T + I_{sc\_STC}) \\ // \exp\left(\frac{N_S (U_{oc\_STC} + K_V \Delta T)}{a N_S U_T}\right) - 1 \end{cases} \quad (4)$$

In (4), at an ambient temperature of  $25^\circ$ , at an effective light irradiance of  $S = 1000W/m^2$  on the PV panel,  $I_{sc\_STC}$  denotes the short-circuit current,  $U_{oc\_STC}$  denotes the open-circuit voltage,  $K_V$  and  $K_i$  represent the voltage temperature coefficient, the current temperature coefficient, and  $S_{STC}$  represents the standard irradiance with a value of  $1000W/m^2$ .

A system based on solar energy generation is known as a PV power generation system. In which a number of internal and external elements in the battery as well as the external environment will have an impact on how the battery is used [11]. The point tracking technology will be accomplished by differentiating the pertinent external environment factors, at which point the maximum electric

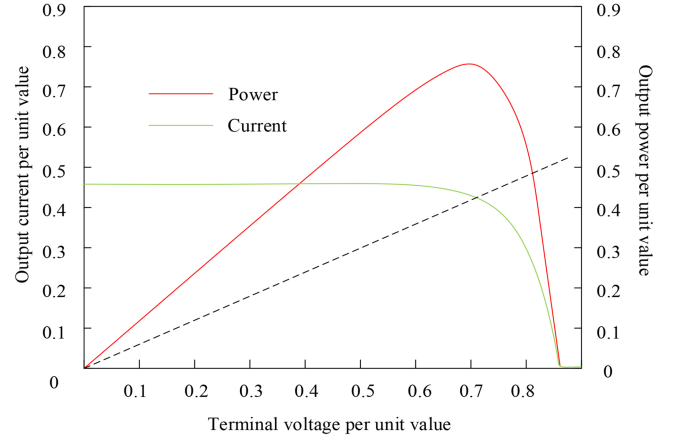


Figure 3. Characteristic curves of current voltage and electric power voltage related to photovoltaic system.

power will result in a significant difference, producing a MPPT technology concept.

As shown in Fig. 3, the characteristic curves of current–voltage and electric power–voltage associated with the PV array are presented [12]. When the PV array’s radiation is stable, a load line can be introduced; the current–voltage curve that intersects the load curve represents the PV array’s output current and voltage. The maximum output voltage and current occur when the internal resistance of the PV system and the corresponding load impedance are equal. This is when the highest power is produced.

A converter known as a DC-DC converter is used to maintain the PV system’s maximum power [13]. The maximum power of the PV system is effectively displayed by the duty cycle property of this converter. In other words, good duty cycle control enables one to understand that the PV system’s maximum power is attained when the voltage and current curves cross.

The PV panel’s solar light signal can be transformed by the DC-DC converter into an electrical signal that is output to the load. Equation (5) illustrates the computations necessary to determine the DC-DC converter’s input voltage and current based on these values.

$$\begin{cases} U_{in} = \frac{U_{out}}{M(d)} \\ I_{in} = M(d) \times I_{out} \end{cases} \quad (5)$$

In (5)  $M(d)$  represents the voltage conversion ratio and  $d$  represents the duty cycle parameter. The upper equation in (5) is divided by the following equation to obtain (6).

$$\begin{aligned} R_{in} &= \frac{U_{in}}{I_{in}} = \frac{U_{out}/M(d)}{M(d) \times I_{out}} \\ &= \frac{1}{M(d)^2} \times \frac{U_{out}}{I_{out}} = \frac{R_{out}}{M(d)^2} \end{aligned} \quad (6)$$

In (6),  $R_{in}$  represents the converter input resistance and  $R_{out}$  represents the converter output resistance.

Equation (6) is equivalent to (7).

$$R_{PV} = \frac{R_{load}}{M(d)^2} \quad (7)$$

In (7), the equivalent resistance of the PV array is represented by  $R_{PV}$ , which also denotes  $R_{in}$  in (6), and  $R_{load}$  represents the load resistance, which is equivalent to  $R_{out}$  in (6). The range of operating point slopes associated with the load is calculated as in (8).

$$\tan \theta = \frac{1}{P_{PV}} = \frac{M(d)^2}{R_{load}} \quad (8)$$

Equation (8) demonstrates how the voltage conversion ratio in the MPPT system is connected to the operating point of the load. When the conversion ratio of the voltage is higher, the higher the value of  $\tan \theta$ , the higher the slope of the load line and the higher the operating point [14], [15].

### 3.2 Fusion of Improved QSA and CIM for Tracking Model Design

One of the optimisation algorithms for particle swarms and a variant based on the particle swarm optimisation algorithm is QSA, which incorporates the concept of quantum computing into the particle swarm optimisation algorithm to improve the convergence performance of the particle swarm optimisation algorithm [16]. The core idea is to represent the particle positions in the particle swarm optimisation algorithm as quantum states and use the idea of quantum computation to update the particle positions, so as to improve the convergence performance of the particle swarm optimisation algorithm. However, there is still a disadvantage in QSA for global optimisation but the algorithm is very slow, this research combines the concept of FL, which is not able to perform global optimisation but the algorithm is fast and compatible and does not reduce the accuracy of the optimisation.

The PV system's voltage and current values are first input into the fuzzy controller for fuzzification, and then, in accordance with the characteristics, the affiliation function is chosen, the pertinent fuzzy rule table is set up, the defuzzification operation is carried out, and the duty cycle of the output response is used as the optimal value [17], [18]. Utilising the Zadeh representation as in (9), the voltage and current received from the PV system are fuzzified.

$$P = \sum_{pv=1}^n \mu_p(I_{pv} \cdot U_{pv}) / I_{pv} \cdot U_{pv} \quad (9)$$

$I_{pv}$  in (9) represents the output current of the PV array and  $U_{pv}$  represents the output voltage. Then, the rule table of fuzzy input and output is set, and the related calculation is shown in (10).

$$\begin{cases} \Delta P_M = -P(k) + P_M(k) \\ \Delta D = -D(k-1) + D(k) \\ \Delta P = -P(k-1) + P(k) \\ \Delta I = -I(k-1) + I(k) \end{cases} \quad (10)$$

In (10),  $\Delta P$  stands for the variation in the PV array's output power,  $\Delta I$  for the variation in output current, and  $\Delta P_M$  for the variation in the collection's maximum and current power points. Positive big, positive small, negative large, and negative small are the fuzzier words for  $\Delta P$  and  $\Delta I$ . Positive big and positive small are the two types of fuzzy terms found in the fuzzy terms of  $\Delta D$ , while positive large, positive medium, and positive small are all found in the fuzzy terms of  $\Delta P_M$ . Negative large, negative medium, and negative small are all present in the fuzzy terms of BBB. 32 FL rules are the result.

According to the corresponding fuzzy rules, the affiliation function needs to be set, and the same triangular affiliation function is used for the fuzzy subsets of the input quantities  $\Delta I$ ,  $\Delta P$ , and  $\Delta P_M$ ; and the triangular affiliation function is used for the fuzzy subsets of the output quantity  $\Delta D$  [19]. Next, defuzzification is required, and the resulting output object is the duty cycle  $\Delta D$ , and the related calculation is shown in (11).

$$\Delta D = \frac{\sum_i^n \mu(D_i) D_i}{\sum \mu(D_i)} \quad (11)$$

$\Delta D$  in (11), which is a collection of discrete numerical values that allows for tracking the MPP by varying the duty cycle. The defuzzification method can be chosen as the discrete domain solution of the centre method. The final output is the amount of change in the optimal duty cycle.

The duty cycle is correlated with the operational voltage in the PV system to build the FL in conjunction with QSA. The output of the PV system *via* the fuzzy FL device, can obtain the optimal duty cycle of the amount of change, *i.e.*, the amount of change in operating voltage, and which the change in voltage of the existence of the maximum and minimum values, in the interval can obtain the corresponding MPP voltage, the pertinent algorithm as (12).

$$\begin{cases} \Delta U = U_0(1 - \Delta D) \\ U_{max} = U_0(1 - \Delta D_{min}) \\ U_{min} = U_0(1 - \Delta D_{max}) \end{cases} \quad (12)$$

In (12),  $\Delta U$  represents the optimal duty cycle variation amount,  $U_{min}$  and  $U_{max}$  represent the minimum and maximum voltage, respectively, and  $U_0$  represents the current measured voltage of the PV array. The maximum power can be found by selecting  $N$  quanta between the variation amount  $[0, U_{oc}]$ , the initial voltage is set to  $U_1 = 0.7U_{oc}$ ,  $U_2 = 0.7U_{oc} + 0.01U_{oc} = 0.71U_{oc}$ , ...,  $U_n = 0.8U_{oc}$ , and the optimisation is performed between the maximum and the minimum voltage. The related optimisation process is shown in Fig. 4.

Variable step size CIM must be used to adjust the DC-DC converter's duty cycle to maximise power point tracking [20]. The variable step-size algorithm is capable of continuously adjusting the duty cycle, is simple to operate, and is the traditional classical algorithm for MPPT technology. The standard variable step-size technique is used to distinguish between the power and voltage ratio

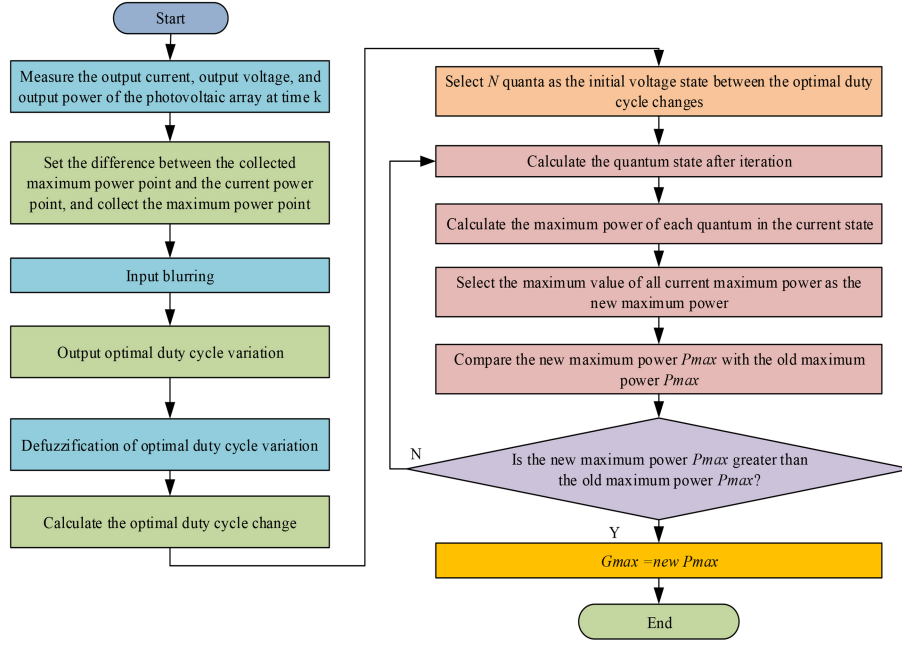


Figure 4. Quantum swarm optimisation combined with fuzzy logic algorithm to optimise the process.

of the PV cell. The outcome is easily influenced by the amount of light present outside, and it is challenging to monitor the maximum power under conditions of extremely unstable light. Equation (13), which depicts the PV cell's output characteristics.

$$\frac{dP}{dU} = \frac{d(UI)}{dU} = I + U \frac{dI}{dU} \quad (13)$$

In (13)  $dP$ ,  $dU$  represent the power and voltage of the PV cell and  $dI$  represents the output current. Equation (13) demonstrates that as a result of a change in light intensity, a change in current will also have a significant impact on the image of the power to voltage ratio of the PV cell. To address this issue, (13)'s power and voltage differentiation will be divided with the current after taking the absolute value, as in (14).

$$S(k) = \frac{1}{I} \left| \frac{dP}{dU} \right| = \left| 1 + \frac{U}{I} \frac{dI}{dU} \right| \quad (14)$$

In (14),  $\frac{U}{I}$  represents the instantaneous amount of resistance and  $\frac{dI}{dU}$  represents the instantaneous increment of conductance. During the process from 0 to maximum power, the value of change in current is very small so that  $\frac{dI}{dU}$  is nearly 0. As the voltage increases,  $\frac{dI}{dU}$  continues to decrease and  $(\frac{U}{I} \frac{dI}{dU})$  is close to 0 in the range, and with the maximum power, the value of  $(\frac{U}{I} \frac{dI}{dU})$  is equal to  $-1$ . The calculations related to the maximum power operation are shown in (15).

$$\begin{cases} \frac{dP}{dU} |_{MPP} = I + U \frac{dI}{dU} = 0 \\ \frac{U}{I} \frac{dI}{dU} |_{MPP} = -1 \end{cases} \quad (15)$$

As the voltage reaches a certain level or even beyond the MPP, the step adjustment factor will then dramatically increase, therefore to assure the algorithm's convergence,

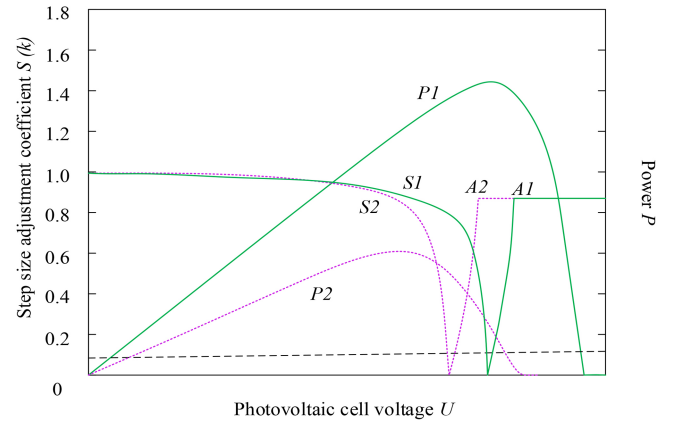


Figure 5. Improved variable step conductance increment technique flowchart.

the step adjustment factor is hereby adjusted as in (16).

$$D(k) = D(k-1) \pm S(k) \Delta D_{ref} \quad (16)$$

In (16),  $S(k)$  represents the step adjustment coefficient,  $D(k)$  represents the reference step value at the moment of  $k$ ,  $D(k-1)$  represents the reference step value at the moment of  $k-1$ , and  $\Delta D_{ref}$  represents the perturbation fixed step. After stipulation, the image change curve of the step adjustment coefficient is shown in Fig. 5.

After combining with the improved variable step-size algorithm, the change of the operating point, the corresponding voltage and current changes are judged, and the maintenance of the steady state is carried out in accordance with the aforementioned improvements to the CIM [21]. This improves the tracking speed and accuracy of the algorithm and the efficiency of power tracking. The flow chart for the enhanced variable step size CIM is shown in Fig. 6.

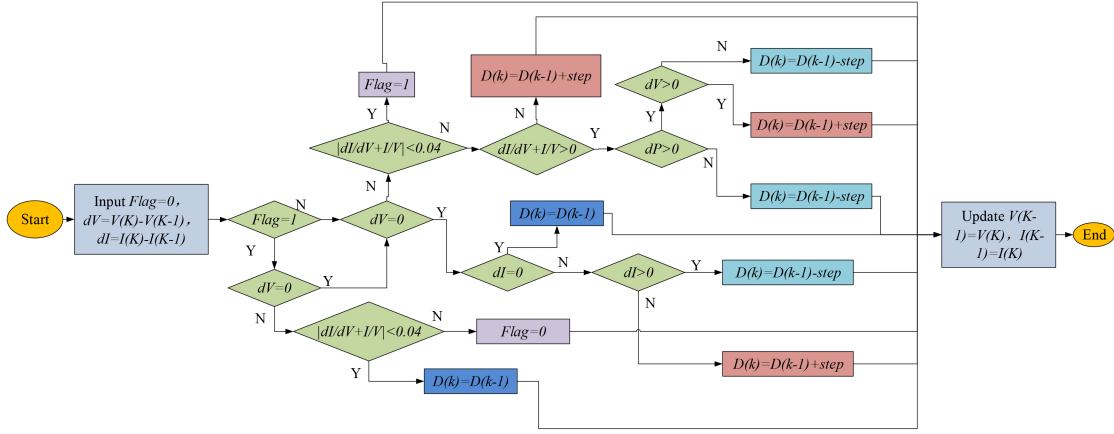


Figure 6. Flowchart of improved variable step conductance increment method.

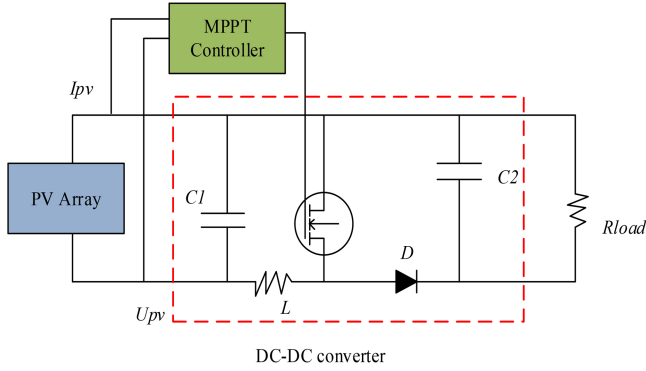


Figure 7. Structural diagram of photovoltaic power generation system.

#### 4. Simulation Experiments of Photovoltaic Power Generation Tracking Model Based on Improved Algorithm

This research addresses the electric power tracking problem of PV power generation, and proposes a new tracking model by combining the improved QSA and CIM. The associated simulation experiments are constructed to test the model's viability and practicability, and the experimental data is then analysed to determine how well the model performed in those tests.

##### 4.1 Simulation Experimental Design

Simulation tests are carried out using MATLAB software to more clearly demonstrate the viability of the PV tracking approach presented in this work. The PV power generation system's structure is schematically depicted in Fig. 7. The PV array, the DC-DC converter circuit and load, as well as the MPPT controller, make up its four components. The converter consists of five parts, such as switch, load, circuit, capacitor, and inductor. The frequency of the switch is set to 20 KHz.

To compare the tracking performance of the traditional CIM and the improved variable step increment method more intuitively and accurately, strong perturbation light

conditions are set up, and the light amplitude of the experiment is increased from 400 W/m<sup>2</sup> to 500 W/m<sup>2</sup> at the moment of 1 s irradiance, and from 500 W/m<sup>2</sup> to 550 W/m<sup>2</sup> at the moment of 2 s. A portion of the experiment is set up as follows to compare the tracking performance of the QSA before and after the upgrade. Part of the experiment was set up so that the temperature was 25° under stable light, 1,000 W/m<sup>2</sup> for series circuit 1 and 500 W/m<sup>2</sup> for series circuit 2. Under unstable light, battery 1 had 1,000 W/m<sup>2</sup> at 0–0.15 s, 375 W/m<sup>2</sup> at 0.15–0.25 s, and 375 W/m<sup>2</sup> at 0.25–0.30 s, the battery power is 650 W/m<sup>2</sup>. Battery 2 has a battery power of 900 W/m<sup>2</sup> at 0–0.15 s, 550 W/m<sup>2</sup> at 0.15–0.25 s and 350 W/m<sup>2</sup> at 0.25–0.30 s.

##### 4.2 Statistical and Econometric Analyses of Experimental Results

The experiment obtained sufficient and credible data information. As shown in Fig. 8, in the experiment, the amplitude of light is directly increased from 200 W/m<sup>2</sup> to 400 W/m<sup>2</sup> at the moment of 1 s, and the simulation results (SR) of the traditional conductivity increment algorithm and the improved conductivity increment algorithm of this research are 0.41 s and 0.32 s, respectively, which is an improvement of 21.95% in tracking speed. The direct increase from 400 W/m<sup>2</sup> to 600 W/m<sup>2</sup> at the moment of 2 s, the SR of the traditional algorithm and the algorithm of this research are 0.46 s, 0.38 s, respectively, and the tracking speed is improved by 17.39%, and the output power of the PV arrays averages 41.52 W and 39.86 W.

The SR of this research algorithm under the micro-turbulent environmental conditions are shown in Fig. 9. The SR can be compared with the strong perturbation condition in Fig. 8. In the two jumps to light amplitude, the average output power of the PV array is 25.16 W and 26.01 W, and the tracking time is reduced from 0.22 s to 0.17 s and from 0.09 s to 0.06 s, and the tracking rate is improved by 22.73% and 33.33%.

According to Table 1, which summarises the changes in tracking times for each magnitude of lighting conditions, the improved CIM with altered step size of this study has the capacity to increase the tracking rate ranging from 15%–25% compared to the traditional CIM, from 400

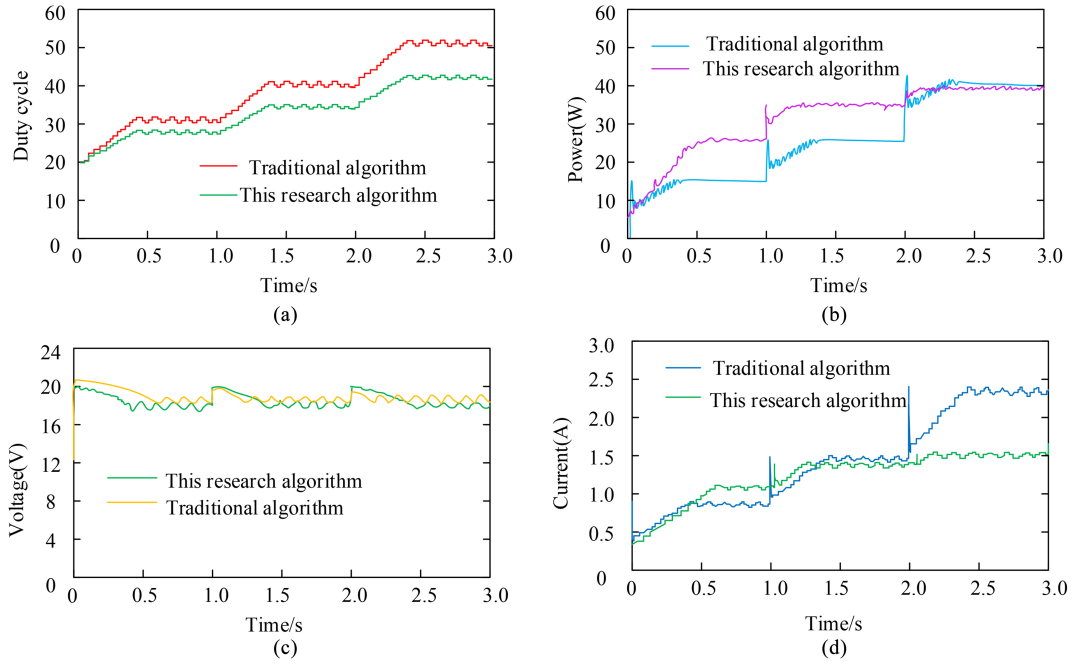


Figure 8. Comparison of SR between traditional algorithms and this research algorithm under strong disturbances: (a) changes in electrical duty cycle; (b) changes in power; (c) voltages changes; and (d) current changes.

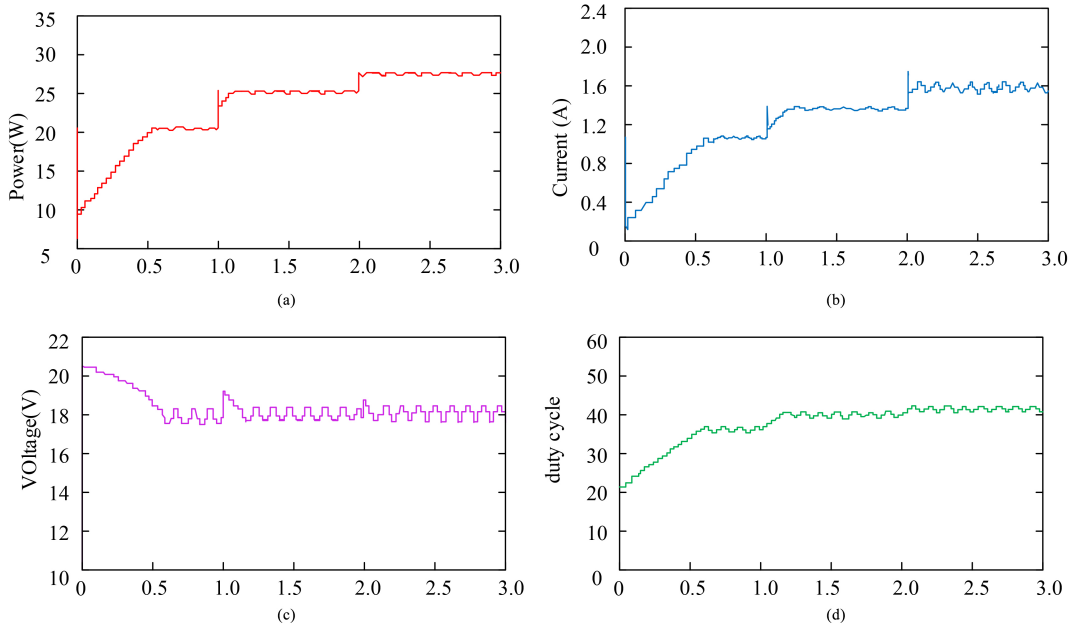


Figure 9. SR of the research algorithm under micro disturbances: (a) electrical power changes; (b) current changes; (c) changes in voltage; and (d) changes in duty cycle.

$W/m^2$  to  $500 W/m^2$ , with the traditional algorithm taking 0.22 s and the algorithm of this study taking 0.17 s, which is an increase in efficiency of 22.73%. From  $500 W/m^2$  to  $550 W/m^2$ , the traditional algorithm takes 0.09 s, and the research algorithm takes 0.06 s, with an efficiency increase of 33.33%. As can be seen, our study algorithm not only addresses the issue of inaccurately estimating irradiance change but also enhances the effectiveness of measuring the maximum power and lowers the time expenditure for system operation.

The electrical power output curves of the quantum swarm optimisation algorithm are depicted in Fig. 10 before and after the enhancement. With the change of environment, the maximum electric power of the improved QSA is 2,920 W, and the maximum electric power of the pre-improved QSA is 2,604 W. It can be seen that, after the improvement of the FL algorithm, although the number of oscillations of the quantum swarm optimisation algorithm has become more frequent, the tracking accuracy is still at a very high level, and it has considerable stability.

Table 1  
Summary of Tracking Time Change Under Each Irradiance

Serial number	Irradiance (kW/m <sup>2</sup> )	Traditional algorithm time (s)	The research algorithm took (s)	Efficiency improvement
1	0.2–0.4	0.41	0.32	21.95%
2	0.4–0.6	0.46	0.38	17.39%
3	0.3–0.4	0.19	0.15	21.05%
4	0.4–0.5	0.22	0.17	22.73%
5	0.5–0.55	0.09	0.06	33.33%

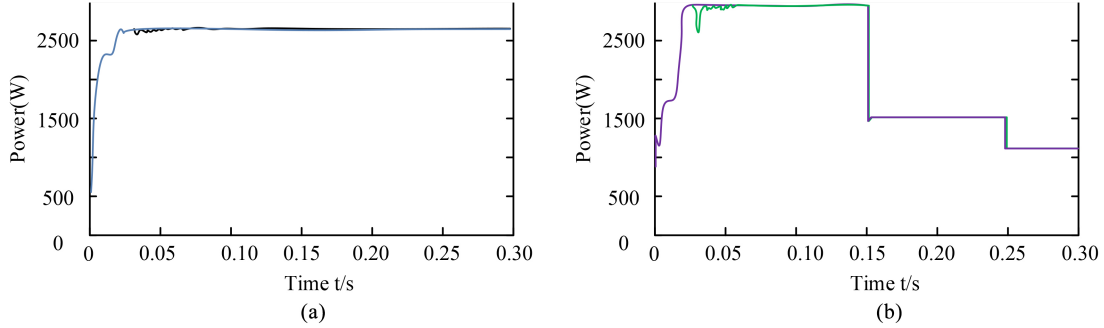


Figure 10. Comparison of quantum swarm optimisation algorithm tracking electric power performance before and after improvement under environmental changes: (a) comparison of tracking performance of quantum swarm optimisation algorithms before and after improvement under stable illumination and (b) comparison of tracking performance of quantum swarm optimisation algorithms before and after improvement under unstable lighting conditions.

To further verify the advantages of the proposed algorithm, the study will use Dagal’s improved Salp swarm optimisation algorithm based on particle swarm optimisation as a comparative algorithm, which is also used to optimise the MPPT point of PV systems. It will be set as the “Comparison algorithm”. As shown in Fig. 11, the output power curves of improved QSA, improved genetic algorithm, and comparative algorithms are studied for tracking performance comparison. From Fig. 11, it can be seen that the maximum electrical power of the improved quantum swarm optimisation algorithm is 2,920 W, the maximum electrical power of the improved genetic algorithm is 2,034 W, and the maximum electrical power of the comparative algorithm is 2,716 W. From this, it can be seen that although the comparison algorithm can also achieve high power, the convergence power achieved is still lower than the improved quantum group algorithm proposed in the study. The optimisation of QSA by FL algorithm reduces the number of iterations, makes the optimisation more accurate, and can obtain a more excellent maximum electrical power optimisation.

## 5. Conclusion

With the goal to track the MPP of the PV cell and maximise PV cell utilisation, this study recommends a special PV power tracking model based on the PV maximum electric power tracking point technique. The FL algorithm is used to optimise the model for QSA,

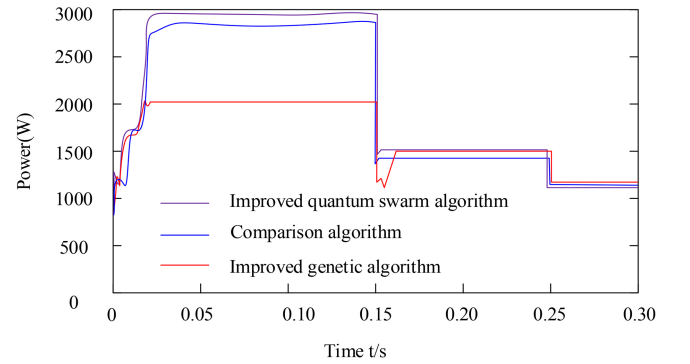


Figure 11. Output power curves of improved quantum swarm algorithm, comparative algorithm, and improved genetic algorithm.

and the traditional CIM is enhanced by adopting an improved variable step size algorithm. The accuracy and tracking rate of the maximum power of PV cells grow as a result of the algorithm’s convergence and rate increasing. To confirm the model’s viability, simulation studies are now conducted. The experiments showed that the pre-improved QSA yielded a maximum electrical power of 1,893 W, while the genetic algorithm yielded a maximum electrical power of 2,034 W, an improvement of 12.13% and 7.45%, respectively. The maximum electrical output of the enhanced QSA is 2,920 W, as opposed to the pre-improved QSA’s 2,604 W maximum, as compared

to the improved genetic algorithm. The improved CIM has the ability to increase the tracking rate by 15% to 25% in contrast to the conventional CIM when exposed to considerable changes in the environment. As can be observed, the combined tracking accuracy and tracking rate of the PV power tracking model using the two upgraded algorithms is exceptional. The stability of the algorithm is still insufficient for the constant voltage algorithm, and the oscillatory nature of the algorithm still needs to be improved over a wide range of numbers, to name a few flaws in this study.

## Fundings

The research is supported by: Research and demonstration of multifunctional scenic spots integrated energy service station based on off-grid photovoltaic power distribution technology.

## References

- [1] I. Dagal, B. Akn, and E. Akboy, Improved Salp swarm algorithm based on particle swarm optimization for maximum power point tracking of optimal photovoltaic systems, *International Journal of Energy Research*, 46(7), 2022, 8742–8759.
- [2] L. Mao, Q. Chen, and J. Sun, Construction and optimization of fuzzy rule-based classifier with a swarm intelligent algorithm, *Mathematical Problems in Engineering*, 2020(Pt.13), 2020, 9319364.1–9319364.12.
- [3] P. Manoharan, U. Subramaniam, S.B. Thanikanti, P. Sanjeevikumer, B.H. Jens, M. Massimo, and R. Sowmya, Improved perturb and observation MPPT technique for solar photovoltaic power generation systems, *IEEE Systems Journal*, 15(2), 2020, 3024–3035.
- [4] A.I.M. Ali and H.R.A. Mohamed, Improved P&O MPPT algorithm with efficient open-circuit voltage estimation for two-stage grid-integrated PV system under realistic solar radiation, *International Journal of Electrical Power and Energy Systems*, 137, 2022, 107805.1–107805.12.
- [5] L. Xu, R. Cheng, and J. Yang, A new MPPT technique for fast and efficient tracking under fast varying solar irradiation and load resistance, *International Journal of Photoenergy*, 2020, 2020, 6535372.1–6535372.18.
- [6] M.A.B. Siddique, A. Asad, R.M. Asif, A.U. Rahman, and I. Ullah, Implementation of incremental conductance MPPT algorithm with integral regulator by using boost converter in grid-connected PV array, *IETE Journal of Research*, 67(1), 2021, 1920481.1–1920481.14.
- [7] J. Mishra, S. Das, D. Kumar, and M. Pattnaik, A novel auto-tuned adaptive frequency and adaptive step: Ize incremental conductance MPPT algorithm for photovoltaic system, *International Transactions on Electrical Energy Systems*, 31(10), 2021, e12813.1–e12813.14.
- [8] Y. Ouberrri, H. Yatimi, and E. Aroudam, Design of a robust sliding mode controller for MPPT based on automation PLC for PV applications, *International Transactions on Electrical Energy Systems*, 30(4), 2020, e12296.1–e12296.19.
- [9] A.F. Mirza, M. Mansoor, K. Zhan, and Q. Ling, High-efficiency swarm intelligent maximum power point tracking control techniques for varying temperature and irradiance, *Energy*, 228, 2021, 120602.1–102602.27.
- [10] G. Hou, Y. Ke, and C. Huang, A flexible constant power generation scheme for photovoltaic system by error-based active disturbance rejection control and perturb & observe, *Energy*, 237, 2021, 121646.1–121646.13.
- [11] S. Motahhir, A. El Hammoumi, and A. El Ghzizal, The most used MPPT algorithms: Review and the suitable low-cost embedded board for each algorithm, *Journal of Cleaner Production*, 246, 2020, 118983.1–118983.17.
- [12] R. Mei and J. Zhang, MPPT algorithm of particle swarm optimization and fuzzy variable step incremental conductance method based on z-source inverter, *Taiyangneng Xuebao/Acta Energiæ Solaris Sinica*, 41(1), 2020, 137–145.
- [13] J. Ahmed, Z. Salam, M. Kermadi, H. Afrouzi, and R. Ashique, A skipping adaptive P&O MPPT for fast and efficient tracking under partial shading in PV arrays, *International Transactions on Electrical Energy Systems*, 11(5), 2021, e13017.1–e13017.24.
- [14] F.U. Khan, M.M. Gulzar, D. Sibtain, H.M. Usman, and A. Hayat, Variable step size fractional incremental conductance for MPPT under changing atmospheric conditions, *International Journal of Numerical Modelling Electronic Networks Devices and Fields*, 33(2), 2020, e2765.1–e2765.18.
- [15] R. Celikel and A. Gundogdu, System identification-based MPPT algorithm for PV systems under variable atmosphere conditions using current sensorless approach, *International Transactions on Electrical Energy Systems*, 30(8), 2020, 1–21.
- [16] A. Chellakhi, S.E. Beid, and Y. Abouelmahjoub, An improved maximum power point approach for temperature variation in pv system applications, *International Journal of Photoenergy*, 2021, 2021, 973204.1–973204.21.
- [17] S. Guo, R. Abbassi, H. Jerbi, A. Rezvani, and K. Suzuki, Efficient maximum power point tracking for a photovoltaic using hybrid shuffled frog-leaping and pattern search algorithm under changing environmental conditions, *Journal of Cleaner Production*, 297, 2021, 126573.1–126573.20.
- [18] L. Xu, R. Cheng, and J. Yang, A new MPPT technique for fast and efficient tracking under fast varying solar irradiation and load resistance, *International Journal of Photoenergy*, 2020, 2020, 6535372.1–6535372.18.
- [19] M. Mao, L. Zhang, L. Yang, B. Chong, H. Huang, and L. Zhou, MPPT using modified Salp swarm algorithm for multiple bidirectional PV-uk converter system under partial shading and module mismatching, *Solar Energy*, 209(1), 2020, 334–349.
- [20] P. Dey and D.K. Jana, Evaluation of the convincing ability through presentation skills of pre-service management wizards using AI via T2 linguistic fuzzy logic, *Journal of Computational and Cognitive Engineering*, 2(2), 2022, 133–142.
- [21] P.A. Ejegwa and J.M. Agbetayo, Similarity-distance decision-making technique and its applications via intuitionistic fuzzy pairs, *Journal of Computational and Cognitive Engineering*, 2(1), 2023, 68–74.

## Biographies



Xuemei Yang was born in November 1984, native to Jingshan, Hubei, Han ethnicity. She received the bachelor's degree in electrical engineering and automation from China Three Gorges University in June 2007, and the master's degree in electrical engineering technology and automation from South China University of Technology in June 2010. Her research direction is new energy generation and grid control technology. She worked as a Dispatcher with the Power Dispatch Communication Center, Tianshui Power Supply Company of Gansu Province Electric Power Company, from August 2010 to September 2011; served as the Protection Specialist with the Dispatching Communication Center of Tianshui Power Supply Company of Gansu Province Electric Power Company from September 2011 to May 2013; served as the Protection Specialist with the Power Dispatch Control Center of Tianshui Power Supply Company of State Grid Gansu Electric Power Company from May 2013 to October 2015; the Deputy Director of the Development

Planning Department of Tianshui Power Supply Company of State Grid Gansu Electric Power Company from October 2015 to May 2017; the Deputy Director of the Marketing Department of Tianshui Power Supply Company of State Grid Gansu Electric Power Company from May 2017 to January 2019; the Director of the Development Planning Department and Party Branch Secretary of Tianshui Power Supply Company of State Grid Gansu Electric Power Company from January 2019 to July 2021; and the Vice General Manager and a Party Committee Member of Wuwei Power Supply Company of State Grid Gansu Electric Power Company since July 2021. She has published multiple academic papers and applied for multiple patents.



*Wenqing Zhang* was born in November 1988, native of Wuwei, Gansu, Han ethnicity. He received the bachelor's degree in electrical engineering and automation from Northeast Electric Power University in 2014. He was the Distribution Network Operation Duty Officer of the distribution emergency repair team with the Wuwei Power Supply Company of State Grid Gansu Electric Power

Company from August 2014 to September 2016; the Office of Wuwei Power Supply Company of State Grid Gansu Electric Power Company was responsible for inspection and supervision from October 2016 to February 2018; served as the Distribution and Maintenance Specialist for the Urban Power Supply Branch of State Grid Gansu Electric Power Company Wuwei Power Supply Company from March 2018 to July 2019; the office of Wuwei Power Supply Company of State Grid Gansu Electric Power Company was responsible for inspection, supervision, and policy research from August 2019 to November 2019; the Deputy Director of the Office of Wuwei Power Supply Company of State Grid Gansu Electric Power Company from December 2019 to March 2022; the Director and the Deputy Secretary of the Urban Power Supply Branch of Wuwei Power Supply Company of State Grid Gansu Electric Power Company from March 2022 to September 2023; and the Director and the Deputy Secretary of the Marketing Department and Branch of Wuwei Power Supply Company of State Grid Gansu Electric Power Company since September 2023. He has applied for two patents and published five papers.



*Wenwen Zou* was born in May 1996, native to Pingliang, Gansu, Han ethnicity. He received the bachelor's degree in electrical engineering and automation from Changsha University of Science & Technology in 2018. From August 2018 to March 2020, he was with the State Grid Wuwei Power Supply Company's Measurement Center's meter installation, power connection,

and collection operation and maintenance team; from March 2020 to May 2021, the person-in-charge of meter installation, power connection, and collection, operation and maintenance work with the Measurement Center of State Grid Wuwei Power Supply Company; from May 2021 to May 2022, the Deputy Director of Xijing Power Supply Station of State Grid Wuwei Power Supply Company (temporary); from May 2022 to October 2023, measurement and collection management (seconded) of the Marketing Department of State Grid Wuwei Power Supply Company; and since October 2023, measurement and collection project management of the Marketing Department of State Grid Wuwei Power Supply Company. He has applied for three patents and published two papers.